Progress In Electromagnetics Research M, Vol. 40, 37–44, 2014

An Efficient Technique for Design of Electrically Thick Differentially-Driven Probe-Fed Microstrip Antennas

Cristiano B. De Paula[1, *], Daniel C. Do Nascimento[2], and Ildefonso Bianchi[2]

Abstract—This paper presents a computationally efficient technique for designing electrically thick differentially-driven rectangular microstrip antennas with coaxial probe feed. It concerns the use of a transmission line model for probe positioning, along with a full-wave field simulator that yields accurate results with reduced number of required full-wave simulations. An electrically thick antenna was designed with the proposed technique to operate at 2442 MHz, having its radiation patterns and input impedance measured and compared against a single-feed rectangular microstrip antenna to demonstrate the advantages of using differential feed to reduce cross-polarization in H-plane.

1. INTRODUCTION

A well-known bandwidth enhancement technique for microstrip antennas is increasing substrate thickness, but single-probe thick microstrip antennas present higher level of cross-polarization in H-plane [1, 2]. In order to suppress cross-polarized components, a differentially-driven microstrip antenna was proposed by [3]. The use of a pair of feed probes excited with currents of equal amplitude and opposite phases contributes to a symmetric radiation pattern in the E-plane [4]. These are advantages in comparison with the single-feed microstrip antenna. Moreover, in the case of a dual-polarization radiator with two pairs of feeds employed, the mutual coupling of each pair of feed is reduced, which results in higher isolation between antenna ports [2]. These characteristics are relevant for a radiator employed as the array element in a sector antenna for mobile communication systems, since these systems usually employ polarization diversity [5].

Recent works developed on differentially-driven microstrip antennas were reported [6–10], and expressions for calculating the input impedance were presented, but none of these works addressed the design of electrically thick antennas using efficiently full-wave field simulators for model optimization. Such works rely mainly on the classical method of cavity model [11], and no expressions for the impedance shift due to probe inductance were presented, though it is known that probe feed presents high inductance in thick substrates [2], making it difficult to match the antenna and its feeding transmission line. Besides, as already pointed out in [12], the use of an approximate method as the cavity model or transmission line model results only in the initial geometry, requiring a full-wave field analysis for model optimization in order to obtain accurate results, which brings the need of having an algorithm for the afterward model optimization, otherwise the design process becomes cumbersome. Therefore, in order to improve the efficiency of computational resources usage by reducing the number of full-wave simulations required to achieve the design goals, it was proposed the use of an adaptive transmission line model for probe-positioning via circuital analysis and an algorithm for its use, along with the full-wave simulator [12]. In the present work, this technique was extended for differentially-driven microstrip antennas and a specific adaptive transmission line model is presented. Finally, an antenna prototype for ISM Band (2.4–2.5 GHz) was constructed and its input reflection coefficient and

Received 3 November 2014, Accepted 26 November 2014, Scheduled 4 December 2014

* Corresponding author: Cristiano Borges de Paula (cborges@cpqd.com.br).

[1] CPqD Research and Development Center in Telecommunications, Brazil. [2] Instituto Tecnológico de Aeronáutica, Brazil.

radiated patterns were measured and compared with those of a single-feed microstrip antenna in order to validate the design technique and highlight the advantages of the differentially-driven microstrip antenna regarding its low cross-polarization in H-plane.

2. DESIGN PROCEDURE

Consider a probe-fed microstrip antenna with a rectangular patch of length L and width W positioned on the surface of a dielectric substrate of thickness h_s, length L_g, width W_g, relative permittivity ε_r and loss tangent $\tan\delta$. The ground plane is underneath the substrate and covers the entire bottom surface, being the impedance reference plane. The geometry is depicted in Figure 1, along with the adopted coordinate system.

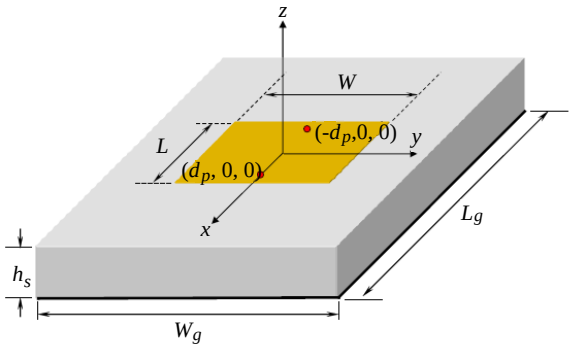

Figure 1. Geometry of the proposed antenna.

The coaxial feed probes are two SMA connectors, not depicted in the figure, positioned underneath the substrate. The center conductors of the SMA connectors are inserted into the substrate and have contact with the patch at coordinates $(d_p,\ 0,\ 0)$ and $(-d_p,\ 0,\ 0)$, where d_p is the probe distance to the patch center. The model optimization process requires scaling the antenna dimensions in order to adjust its center frequency, which makes it convenient to write both the probe position and the patch width as functions of the patch length [12]. Hence, the probe distance d_p can be written as

$$d_p = R_p L, \quad 0 < R_p \leq 0,5, \tag{1}$$

and the patch width can be written as

$$W = RL, \quad R \geq 1, \tag{2}$$

where R_p is the control variable that sets the positions of probes, and R is the control variable that sets the desired geometry of the patch (square, rectangular). Microstrip antennas constructed for this work presented rectangular patch shape with $R = 1.3$.

During the model design optimization, variable L is adjusted to tune the antenna (change its center frequency) and R_p is adjusted to match it, i.e., minimize the reflection coefficient magnitude at the input ports of the antenna.

For the initial geometry, $R_p = 0.25$ and the patch length is

$$L_1 = \frac{c_0}{2f_0\sqrt{\varepsilon_r}}, \tag{3}$$

where the index 1 indicates the first iteration of a series of L values during model optimization, c_0 is the speed of the light in free space and f_0 is the antenna desired center frequency.

Considering that the antenna has two feed probes, it is a 2-port device, and it can be described by its impedance matrix obtained by full-wave simulation,

$$\begin{bmatrix} V_1 \\ V_2 \end{bmatrix} = \begin{bmatrix} Z_{11} & Z_{12} \\ Z_{21} & Z_{22} \end{bmatrix} \begin{bmatrix} I_1 \\ I_2 \end{bmatrix}, \tag{4}$$

where V_1 and V_2 are the voltages, and I_1 and I_2 are the currents of antenna coaxial feed probes at the reference plane. Since the antenna model is symmetric resulting $Z_{11} = Z_{22}$, $[Z]$ corresponds to a reciprocal network that yields $Z_{12} = Z_{21}$, and the antenna will be fed differentially, i.e., $I_1 = -I_2$, the active input impedance is the same in both coaxial feed probes at the reference plane and can be written as

$$Z_i = Z_{11} - Z_{12}. \tag{5}$$

It is considered that the antenna feeding network will be implemented by a 3 dB 180° hybrid coupler, Balun, or power splitter to feed both probes with equal amplitude and opposite phases through transmission lines with convenient lengths and characteristic impedance Z_0. Thus, probes positions need to be adjusted through proper control of the variable R_p in order to match each feed probe to its respective transmission line. The magnitude of the active reflection coefficient for each probe at reference plane is written as

$$|\Gamma| = \left| \frac{Z_i - Z_0}{Z_i + Z_0} \right|. \tag{6}$$

For the sake of simplicity, considering an ideal 3 dB 180° hybrid coupler as the feeding network, it can be easily calculated that the magnitude of reflection coefficient at the Δ port of the coupler when both coupled ports are terminated on Z_i impedances yields $|\Gamma|$. Therefore, it is possible to consider the reflection coefficient of a single port during the design of the antenna as the one that would be obtained from the differentially-driven microstrip antenna with its feeding network. If the antenna is directly fed by a balanced circuit, the differential impedance is twice Z_i, since Z_i is the impedance relative to ground.

In order to reduce the number of full-wave simulations and save computer resources, probe positioning is performed only using circuital analysis. This is accomplished by using a circuital model that can predict the active impedance locus for different probe positions and it will be described in the next session. At this point, it is necessary to define the resonant frequency f_r since electrically thick microstrip antennas may not present a null reactance [1]. The same definition as that used by [12] will be adopted here, which can be written as

$$|\Gamma(f_r)| = \min_f |\Gamma(f)| \quad \text{for} \quad f \in [f_1, f_2], \tag{7}$$

where $[f_1,\ f_2]$ is the frequency range of both full-wave and circuital simulations. For electrically thick microstrip antennas, the simulation frequency range has been set to $[0.8f_0,\ 1.2f_0]$. The goal of probe positioning is to adjust R_p such as $|\Gamma(f_r)| \leq \Gamma_{\min}$, where $\Gamma_{\min}$ is a desired specification, e.g., it may be specified that $|\Gamma(f_r)| \leq -30$ dB. But, despite the fact the antenna is matched after tuning R_p, f_r may be different from the desired value f_0, thus patch length scaling is performed by a factor given by f_r/f_0 until the resonance frequency offset is within given specification limits. Every time a patch scaling is performed, a new full-wave simulation is executed for verification, and if needed, a new iteration of the algorithm is performed.

3. ADAPTIVE TRANSMISSION LINE MODEL (ATLM)

The circuital model used to predict the active antenna impedance locus is shown in Figure 2. It is composed by a generator with impedance Z_g, a capacitor with capacitance C, an ideal transmission line TL with characteristic impedance Z_p and electrical length (in degrees) given by

$$\angle E_l = 360 h_s \left(\frac{c_0}{f\sqrt{\varepsilon_r}} \right)^{-1}, \tag{8}$$

where f is the simulated frequency, a first microstrip μS_1 with length $L_{\mu 1}$ and width $W_{\mu 1}$, a second microstrip μS_2 with length $L_{\mu 2}$ and width $W_{\mu 2}$ and a load L_f that is defined by its reflection coefficient Γ_f written as

$$\Gamma_f = (a_0 + a_1 f) e^{-j(b_0 + b_1 f)}, \tag{9}$$

where the constants a_0, a_1, b_0 and b_1 are derived during the circuit model synthesis.

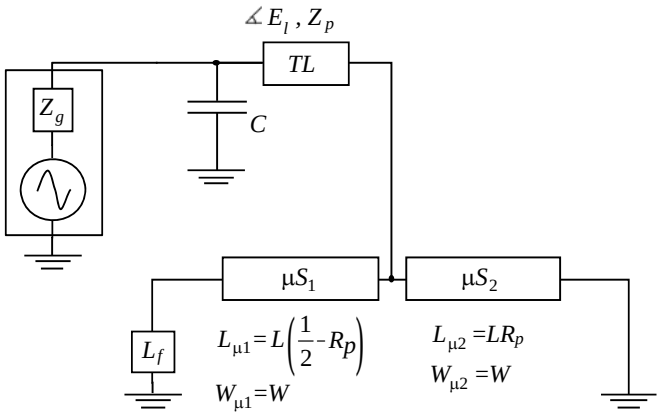

Figure 2. Adaptive transmission line model for the differentially-driven microstrip antenna.

In order to possibly use this model to adjust R_p and make $|\Gamma(f_r)| \leq \Gamma_{\min}$, first it is necessary to synthesize it to obtain an accurate impedance locus. This can be accomplished using a Gradient optimization tool, usually available in circuit simulators, to calculate C, Z_p and the constants a_0, a_1, b_0 and b_1 to fit the circuital model impedance locus to the one obtained in the full-wave simulation. Since the circuital model adapts its input impedance to fit the one from full-wave simulation, it is an adaptive model per nature and it was named ATLM — Adaptive Transmission Line Model [12]. Initial values are: $a_0 = 0.5$, $a_1 = 0\,\mathrm{s}$, $b_0 = 0.5$, $b_1 = 0\,\mathrm{s}$, $Z_p = 100\,\Omega$, $C = 0\,\mathrm{pF}$ and R_p is set to the same value used on the full-wave simulation model. During the synthesis, the generator impedance is given by

$$Z_g = Z_i^*, \tag{10}$$

where the superscript $*$ denotes the complex conjugate operator, and Z_i is the full-wave simulation active impedance. The same goals used by [12] for the circuital model synthesis are used here. They are the following:

$$\mathrm{Re}\{Z_f\} > 0, \tag{11}$$

$$\mathrm{Im}\{Z_f\} < 0, \tag{12}$$

where Z_f is the impedance of the load L_f and

$$|\Gamma| \leq \begin{cases} -30\,\mathrm{dB}, & f \in \left[\left(f_0 - \dfrac{f_2 - f_1}{4}\right), \left(f_0 + \dfrac{f_2 - f_1}{4}\right)\right] \\ -20\,\mathrm{dB}, & f \notin \left[\left(f_0 - \dfrac{f_2 - f_1}{4}\right), \left(f_0 + \dfrac{f_2 - f_1}{4}\right)\right] \end{cases}. \tag{13}$$

Goals (11) and (12) are constraints in order to obtain a solution meaningful from a physical standpoint, if we consider that the load L_f corresponds to an equivalent slot located at the patch edge, and impedance Z_f is the radiation impedance, similar to the previously proposed transmission lines models [13, 14], in which the slot admittance was employed and calculated by approximated expressions. Goal (13) defines the level of accuracy desired between simulated impedance locus from circuital model and full-wave data, since in practice it is difficult to obtain equal impedance loci with both models.

Once the constants a_0, a_1, b_0, b_1 and parameters C and Z_p are calculated and the generator impedance is changed such as $Z_g = Z_0$, the circuital model is able to predict with high level of accuracy the impedance locus that would be obtained if the probe position varied in the full-wave model, which is the key feature that allows one to use the circuital model to optimize R_p instead of running additional full-wave simulations.

When adjusting R_p in the circuital model to make $|\Gamma(f_r)| \leq \Gamma_{\min}$ it can be noticed that f_r changes as well. After finding the desired R_p value, f_r is used for patch length scaling, and a new full-wave simulation must be done for result verification.

4. ANTENNA DESIGN

To illustrate the design technique, one differentially-fed rectangular microstrip antenna was designed and a prototype was built for operation at center frequency $f_0 = 2442\,\text{MHz}$. It was specified a fractional impedance bandwidth of at least 5% for VSWR ≤ 2. It was decided to use the Arlon® CuClad 250 GX substrate, whose characteristics are $\varepsilon_r = 2.55$, loss tangent $\tan\delta = 0.002$ and height $h_s = 6.35\,\text{mm}$. At resonance, the maximum admissible magnitude of reflection coefficient was $-30\,\text{dB}$, i.e., $\Gamma_{\min} = -30\,\text{dB}$, and the maximum frequency error allowed for the final iteration of the algorithm was 0.25%. Antenna feed network characteristic impedance is $Z_0 = 50\,\Omega$. Antenna dimensions are $L_g = W_g = 100\,\text{mm}$ and coaxial probe feeds are two SMA connectors. With this set of specifications, an initial model was simulated in MWS CST® software, a full-wave field simulator, with $R = 1.3$, $L_1 = 38.47\,\text{mm}$, $R_{p1} = 0.25$, in which indexes indicate the first iteration of the algorithm. With these parameter values, one can observe $|\Gamma(f_r)| = -16.6\,\text{dB}$. This result is shown in Figure 3.

Because at the first iteration of the design $|\Gamma(f_r)| > \Gamma_{\min}$ probe positioning was required and the ATLM was synthesized with $L_1 = 38.47\,\text{mm}$ and $R_{p1} = 0.25$, since the ATLM must be synthesized with the same antenna dimensions used for full-wave simulation. Its parameters were derived using a Gradient optimization tool, available at Agilent ADS® software, a circuit simulator, and the following parameter set was found: $C = 0.21\,\text{pF}$, $Z_p = 99\,\Omega$, $a_0 = 0.60$, $a_1 = 6.83 \times 10^{-11}\,\text{s}$, $b_0 = -0.72$ and $b_1 = 7.65 \times 10^{-11}\,\text{s}$. As shown in Figure 4, the active impedance locus obtained by circuital simulation fits very well the active locus from full-wave data. Then, probe positioning was done using the ATLM resulting $R_{p2} = 0.21$, $f_r = 2225\,\text{MHz}$ and $|\Gamma(f_r)| = -34\,\text{dB}$. With this resonance frequency, patch length scaling was done by a factor of 0.911, resulting $L_2 = 35.05\,\text{mm}$. As the patch length was changed, a new full-wave simulation was done after updating model parameters. It was found $|\Gamma(f_r)| = -39\,\text{dB}$ at $f_r = 2408\,\text{MHz}$, hence antenna matching was according the desired specification and probe positioning was not required, but resonance frequency was offset by $-34\,\text{MHz}$, which yields a frequency error of 1.4%, higher than the admissible value. Therefore another patch length scaling was needed, resulting $L_3 = 34.56\,\text{mm}$.

A third iteration full-wave simulation of the design algorithm yielded $|\Gamma(f_r)| = -34\,\text{dB}$ at $f_r = 2438\,\text{MHz}$, which meets all design requirements. The prototype was constructed based on the dimension values obtained from the design, and presented $f_r = 2424\,\text{MHz}$, $|\Gamma(f_r)| = -35\,\text{dB}$, in addition to a fractional bandwidth of 7% (BW = 169 MHz). The active impedance was calculated based on its Z parameters (derived from its measured S parameters) using (5).

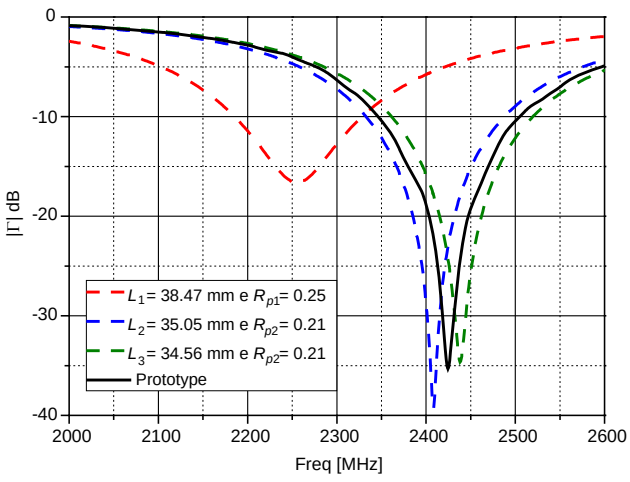

Figure 3. Magnitude of reflection coefficient of full-wave simulations and experimental data based on active impedance Z_i.

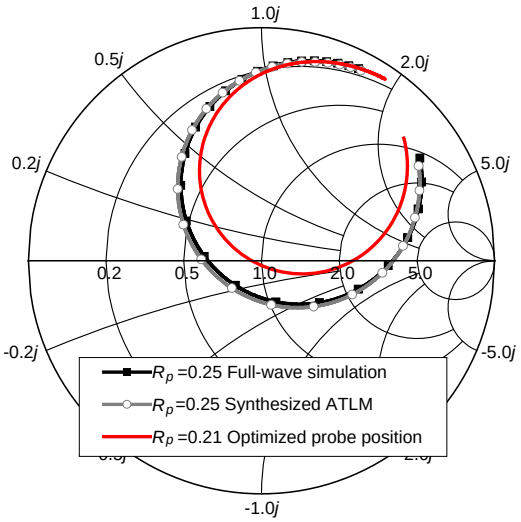

Figure 4. Active impedance loci of circuital and full-wave simulations.

5. EXPERIMENTAL RADIATED RESULTS AND DISCUSSION

In order to demonstrate the advantage of using differential feed to reduce the cross-polarization level in H-plane, a second antenna was used as reference. This antenna was fabricated on the same substrate, but it is a single-feed rectangular microstrip antenna with the following parameters: $L = 34.79\,\text{mm}$, $R_p = 0.34$, $L_g = W_g = 100\,\text{mm}$, $R = 1.3$. It was designed to have the same center frequency, and the measured magnitude of reflection coefficient was $|\Gamma(f_r)| = -31\,\text{dB}$ at $f_r = 2427\,\text{MHz}$. Its fractional bandwidth is 7% [15]. Prototypes of differentially-driven and single-probe antennas are shown on Figure 5. As one can observe, the single-probe microstrip antenna, designed to operate at the same frequency as that of the differentially-driven antenna, has a probe positioned farther from the center of the patch. This implies that, as the substrate is made thicker, and consequently the impedance locus shift is more pronounced and more inductive, the probe will approach the edge of the patch first for the single-probe microstrip antenna. As a result, antenna matching will not be possible, first for the single-probe and followed by the differential feeding technique, therefore it is possible to use thicker substrates for differentially-driven microstrip antennas and obtain improved impedance bandwidth.

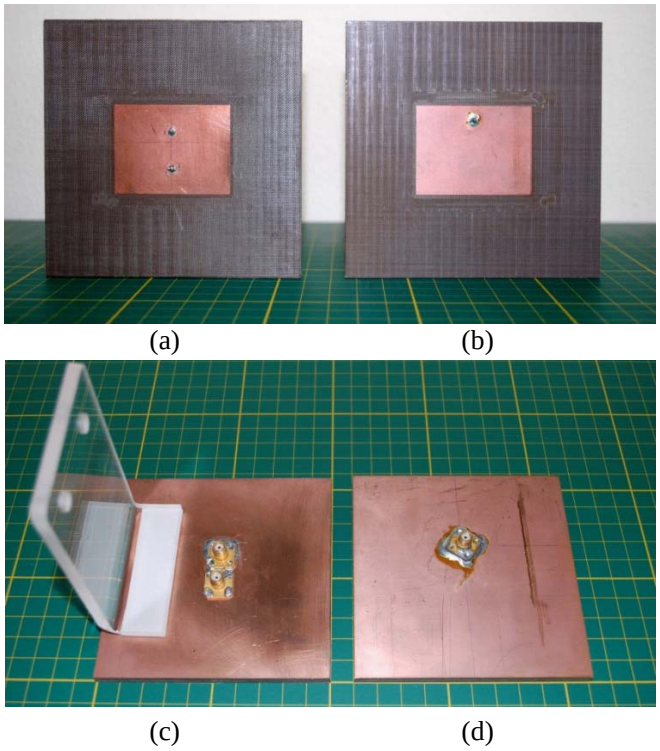

Figure 5. Prototypes: (a), (c) differentially-driven microstrip antenna, (b), (d) single-probe microstrip antenna.

The differentially-driven antenna required a feeding network that was constructed with a Mini-circuits® power splitter (ZAPD-4-N+) and RG 223/U cables with different lengths to ensure 180° phase difference at the antenna coaxial feeds. Measured phase unbalance was 2° and amplitude unbalance was 0.1 dB at 2442 MHz. Insertion loss between the common port and the first antenna port was 4.30 dB and between the common port and the second antenna port was 4.20 dB. Thus, the feeding network presented a differential insertion loss of 1.24 dB.

The radiated patterns obtained with full-wave simulation are shown on Figure 6. Crosspolar simulated radiated pattern of differentially-driven microstrip antenna was lower than −60 dB considering an ideal differential lossless feeding network. The measured copolar radiated patterns are shown in Figure 7. Both antennas present very similar patterns for front radiation, with a noticeable improvement

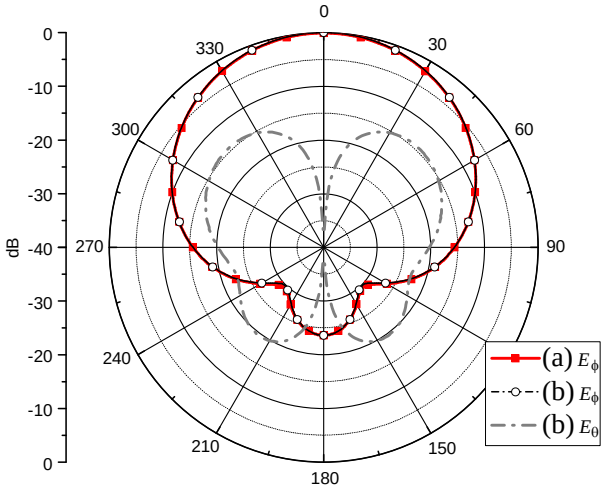

Figure 6. Full-wave simulation radiated patterns for copolar (E_ϕ) and crosspolar (E_θ) fields in H-plane (plane YZ) at 2442 MHz: (a) differentially-driven microstrip antenna, (b) single-probe microstrip antenna.

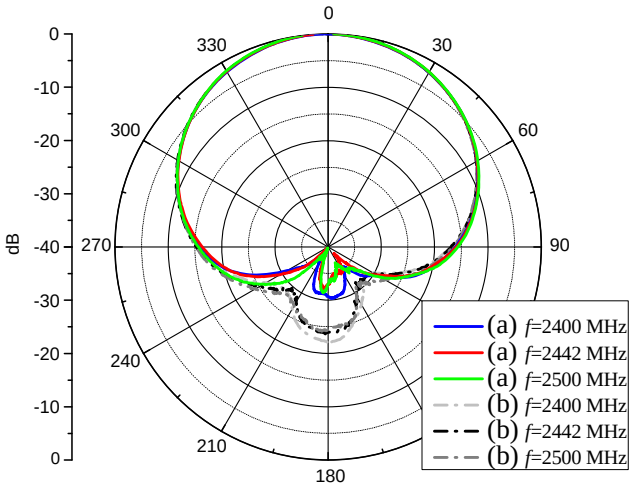

Figure 7. Measured copolar (E_ϕ) radiated patterns in H-plane (plane YZ): (a) differentially-driven microstrip antenna, (b) single-probe microstrip antenna.

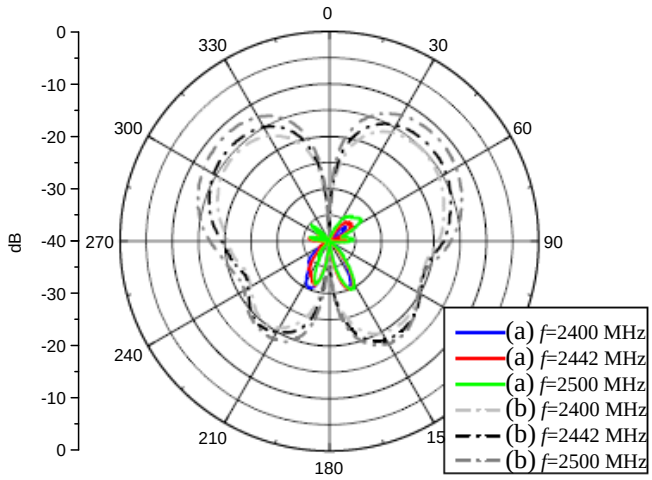

Figure 8. Measured crosspolar (E_θ) radiated patterns in H-plane (plane YZ): (a) differentially-driven microstrip antenna, (b) single-probe microstrip antenna.

of the front-to-back ratio for the differentially-driven antenna. Antenna gain at 2442 MHz was 7.3 dBi and 8.3 dBi for differentially-driven and single-probe types, respectively (measurement uncertainty was 0.9 dB for the anechoic chamber used). The observed difference of gain may be attributed to the feeding network used for the differentially-driven microstrip antenna.

Considering the crosspolar radiated patterns as shown in Figure 8, there is a very high improvement in cross-polarization between the differentially-driven and the single-probe microstrip antennas. The former has a maximum cross-polarization value of -29.7 dB at 2500 MHz, and the latter -11.5 dB at 2500 MHz, thus an experimental improvement of 18.2 dB was observed.

6. CONCLUSION

An efficient technique for designing electrically thick differentially-driven probe-fed microstrip antennas was presented, and a prototype with 7% fractional bandwidth was designed with the proposed technique, having its radiated patterns measured and compared with those of a conventional single-probe microstrip antenna. The design was proved to be computationally efficient as it required only three full-wave simulations in order to achieve the desired goals. Additionally, based on the comparison of the differentially-driven and conventional single-probe antenna designs it was found that differential feeding technique allows the design of thicker matched antennas. Such a conclusion is due to the fact that in single-probe microstrip antennas, the probe is located farther from the center of the patch, which becomes a limitation for antenna matching as substrate height is increased. Finally, the radiated patterns in H-plane for the differentially-driven antenna showed a significant cross-polarization reduction of 18.2 dB.

REFERENCES

1. Chang, E., S. A. Long, and W. F. Richards, "An experimental investigation of electrically thick rectangular microstrip antennas," *IEEE Trans. Antennas Propag.*, Vol. 34, No. 6, 767–772, Jun. 1986.
2. Huang, J., "Microstrip antennas: Analysis, design, and application," *Modern Antenna Handbook*, 157–200, C. A. Balanis (ed.), Wiley, Hoboken, 2008.
3. Chiba, T., Y. Suzuki, and N. Miyano, "Suppression of higher modes and cross polarized component for microstrip antennas," *IEEE Antenna and Propagation Society Int. Symp.*, Vol. 2, 285–288, Albuquerque, Piscataway, 1982.
4. Petosa, A., A. Ittipiboon, and N. Gagnon, "Suppression of unwanted probe radiation in wideband probe-fed microstrip patches," *Electronics Letters*, Vol. 35, No. 5, 355–357, Mar. 1999.
5. Fujimoto, K., "Antennas for mobile communications," *Modern Antenna Handbook*, 1143–1228, C. A. Balanis, Ed., Wiley, Hoboken, 2008.
6. Zhang, Y. P. and J. J. Wang, "Theory and analysis of differentially-driven microstrip antennas," *IEEE Trans. Antennas Propag.*, Vol. 54, No. 4, 1092–1099, Apr. 2006.
7. Zhang, Y. P., "Design and experiment on differentially-driven microstrip antennas," *IEEE Trans. Antennas Propag.*, Vol. 55, No. 10, 2701–2708, Oct. 2006.
8. Zhang, Y. P., "Electrical separation and fundamental resonance of differentially-driven microstrip antennas," *IEEE Trans. Antennas Propag.*, Vol. 59, No. 4, 1078–1084, Apr. 2011.
9. Tong, Z., A. Stelzer, and W. Menzel, "Improved expressions for calculating the impedance of differential feed rectangular microstrip patch antennas," *IEEE Microw. Wireless Compon. Letters*, Vol. 22, No. 9, 441–443, Sep. 2012.
10. Zhang, Y. P. and Z. Chen, "The Wheeler method for the measurement of the efficiency of differentially-driven microstrip antennas," *IEEE Trans. Antennas Propag.*, Vol. 62, No. 6, 3436–3439, Jun. 2014.
11. Richards, W. F., Y. T. Lo, and D. D. Harrison, "An improved theory for microstrip antennas and applications," *IEEE Trans. Antennas Propag.*, Vol. 29, No. 1, 38–46, Jan. 1981.
12. Ferreira, D. B., C. B. de Paula, and D. C. do Nascimento, "Design techniques for conformal microstrip antennas and their arrays," *Advancement in Microstrip Antennas with Recent Applications*, 3–31, A. Kishk, Ed., InTech, Rijeka, 2013, Doi: 10.5772/53019.
13. Munson, R. E., "Conformal microstrip antennas and microstrip phased arrays," *IEEE Trans. Antennas Propag.*, Vol. 22, No. 1, 74–78, Jan. 1974.
14. Derneryd, A. G., "A theoretical investigation of the rectangular microstrip antenna," *IEEE Trans. Antennas Propag.*, Vol. 26, No. 4, 532–535, Jul. 1978.
15. De Paula, C. B., D. B. Ferreira, and I. Bianchi, "Algorithm for the design of linearly polarized microstrip antennas," *Momag Symp.*, João Pessoa, Brazil, Aug. 5–8, 2012 (in Portuguese).